Available online at www.sciencedirect.com

SCIENCE DIRECT®

Journal of Molecular Catalysis A: Chemical 198 (2003) 185–194

JOURNAL OF MOLECULAR CATALYSIS A: CHEMICAL

www.elsevier.com/locate/molcata

Kinetic and FT-IR study for the mechanism of addition of hydrogen sulfide to methyl acrylate over solid basic catalysts

Emmanuelle Breysse[a], François Fajula[a], Annie Finiels[a], Georges Frémy[b], Jean Lamotte[c], Françoise Maugé[c], Jean-Claude Lavalley[c], Claude Moreau[a,*]

[a] *Laboratoire de Matériaux Catalytiques et Catalyse en Chimie Organique, UMR ENSCM-CNRS 5618, Ecole Nationale Supérieure de Chimie, 8, Rue de l'Ecole Normale, 34296 Montpellier Cedex 5, France*

[b] *Groupement de Recherches de Lacq ATOFINA, BP 34, 64170 Lacq, France*

[c] *Laboratoire de Catalyse et Spectrochimie, UMR ISMRA-CNRS 6506, Institut des Sciences de la Matière et du Rayonnement, 6, Boulevard du Maréchal Juin, 14050 Caen Cedex, France*

Received 22 July 2002; accepted 2 December 2002

Abstract

Addition of H_2S to methyl acrylate was performed in a batch reactor at 413 K, 400 rpm and at different concentrations in methyl acrylate and H_2S in the presence of a commercially available mixed magnesium–aluminum basic oxide, namely the KW 2200 catalyst. Under chemical regime, the rate law was shown to follow a "poisoned" Eley–Rideal mechanism in which H_2S reacts in the adsorbed state, whereas methyl acrylate, also capable of being adsorbed on the catalyst, would react in a physisorbed state.

FT-IR study of methyl acrylate and H_2S adsorption performed on MgO are in agreement with these kinetic results. Co-adsorption experiments showed that both methyl acrylate and H_2S were strongly adsorbed on MgO. By varying the order of introduction of the two reactants, i.e. adsorption of H_2S followed by methyl acrylate addition or methyl acrylate adsorption followed by H_2S addition, it was shown that chemisorbed H_2S species like HS^- species which result from H_2S dissociative adsorption were the active species and that strongly adsorbed methyl acrylate was not involved in the reaction.

Keywords: Aldolisation; Michael addition; Base catalysis; IR spectroscopy

1. Introduction

The nucleophilic Michael-type reaction addition of H_2S to methyl acrylate (MA, Eq. (1), Scheme 1) to yield methyl 3-mercaptopropionate (MMP, Eq. (1), Scheme 1) over solid basic catalysts has already been studied, mainly in the patent literature [1,2]. Then, methyl 3-mercaptopropionate can react with methyl acrylate to lead to the formation of dimethyl 3,3′-thiodipropionate (DMTDP, Eq. (2), Scheme 1). Moreover, other side-reactions may take place, namely condensation of two molecules of methyl 3-mercaptopropionate to give the corresponding disulfide and polymerization of methyl acrylate.

The activity of the catalyst can be related to its ability to form reactive nucleophilic species HS^- and consequently to its basic character. However, a high selectivity to methyl 3-mercaptopropionate (MMP) is

* Corresponding author. Tel.: +33-4-67-163-459; fax: +33-4-67-163-470.
E-mail address: cmoreau@cit.enscm.fr (C. Moreau).

1381-1169/02/$ – see front matter © 2002 Elsevier Science B.V. All rights reserved.
doi:10.1016/S1381-1169(02)00690-8

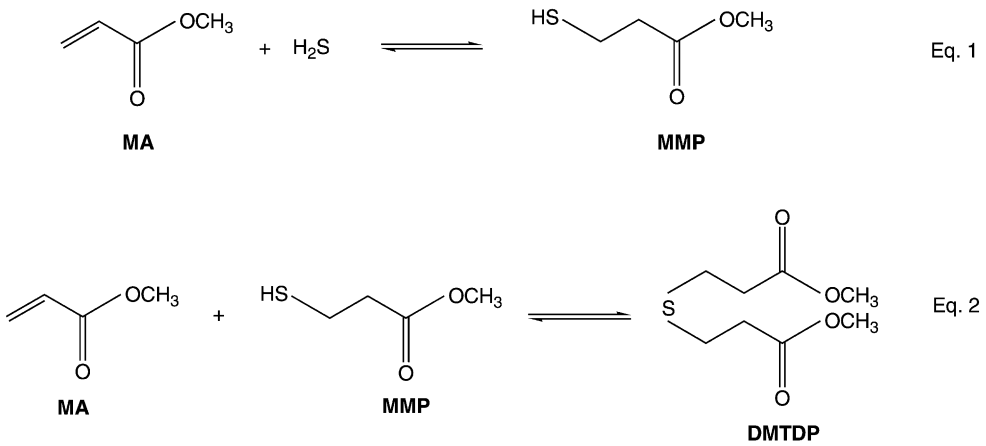

Scheme 1. Reaction scheme for base-catalyzed addition of H_2S to methyl acrylate.

generally achieved in the presence of a large excess of H_2S, whatever the catalysts used: magnesium oxide [1], anionic-exchanged resins [2].

The purpose of this work is to determine the mechanism of this reaction and to propose a kinetic model available for the commercial basic solid KW 2200 catalyst. Therefore, we investigated more deeply the effect of all parameters capable of influencing the course of the reaction. In parallel, an infrared study was performed in order to specify the interaction of the reactants with the catalyst and to determine active species. The IR study was done using magnesium oxide as catalyst, due to its higher transparency than a mixed magnesium–aluminum oxide to the IR beam in the range below 1200 cm^{-1}.

2. Experimental part

2.1. Reactants

Methyl acrylate (99% purity) was from Aldrich, decane (solvent) and dodecane (internal standard) from Interchim, and hydrogen sulfide (99.8% purity) from Aga.

2.2. Catalysts

Mixed magnesium–aluminum oxides used in this work were KW 2000 and KW 2200 from Kyowa with an aluminum molar fraction of 0.3 and particle sizes of 70 and 1.7 μm, respectively. They were calcined at 450 °C prior to use. Catalyst weights mentioned in this paper are those after activation procedure. Specific surface areas measured are 240 and 160 $m^2\,g^{-1}$, respectively. Magnesium oxide was prepared from the brucite-like magnesium hydroxide from Strem Chemical. It was calcined overnight at 823 K, in air.

2.3. Procedure

All reactions were conducted in a jacketed 0.1 l magnetically stirred autoclave (Autoclave Engineers) containing 50 ml of solution. The reactor was fitted with a six-bladed, 2 cm diameter impellers.

In a typical run, the autoclave was charged with a mixture of 10^{-2} mol of methyl acrylate, and 5×10^{-3} mol of dodecane as the internal standard in 50 ml of decane, and 88 mg of freshly activated catalyst. The reactor was closed, purged with nitrogen and cooled at 273 K. Then, H_2S gas was introduced to the required pressure level and the reactor was heated to 313 K.

2.4. Analyses

Samples were periodically withdrawn and analyzed by gas–liquid chromatography (Hewlett-Packard 6890

gas chromatograph equipped with a flame ionization detector, HP5-capillary column 30 m × 0.32 mm, 0.25 μm film thickness, hydrogen as carrier gas), 40–523 K, 30 K min^{-1}.

The initial reaction rates were deduced from the experimental curves of concentration versus time by determination of the slope at the origin.

2.5. IR measurements

FT-IR spectra were recorded with a Nicolet 560 spectrometer. MgO was pressed under the form of a disk (diameter = 16 mm; mass ∼ 15 mg). The pellet was activated by heating under primary vacuum overnight at 653 K followed by heating at 773 K for 1 h under secondary vacuum. Methyl acrylate and H_2S adsorption experiments were performed at 313 K and the spectra were recorded at this temperature. Two different kinds of experiments were performed according to whether H_2S adsorption was followed by MA addition, or MA adsorption was followed by H_2S addition. In any case, the spectrum of the activated MgO was automatically subtracted in order to obtain that of the adsorbed species.

3. Results and discussion

3.1. Reaction scheme

A typical concentration versus time profile is presented in Fig. 1. This figure shows the disappearance of methyl acrylate and appearance of the various identified products (methyl 3-mercaptopropionate, dimethyl 3,3′-thiodipropionate and traces of disulfide) as a function of time. As it might be expected, the selectivity to methyl 3-mercaptopropionate decreases linearly with increasing methyl acrylate conversion, from 71% for a conversion of 18–57% for a conversion of 80%.

3.2. Kinetic study

The addition of H_2S on methyl acrylate was systematically investigated by studying the effect of various parameters on the initial reaction rates and then the data were analyzed for discrimination between different rate models.

Experiments are carried out in a mechanically agitated slurry reactor. Due to the heterogeneous nature of the three-phase system (gas–liquid–solid), a

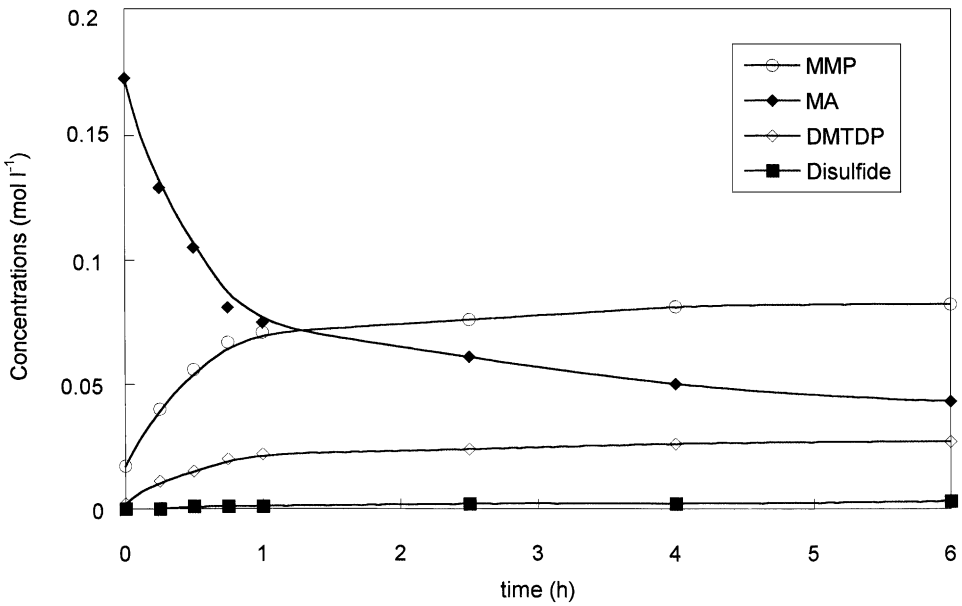

Fig. 1. Typical concentration vs. time profile for addition of H_2S to methyl acrylate in the presence of hydrotalcite catalyst.

number of steps have to occur before reactants can be converted to products. The major steps are: (i) mass transfer of H_2S from gas phase to the bulk liquid, (ii) mass transfer of reactants from bulk liquid to the catalyst surface, (iii) intraparticle diffusion of the reactants within the pores of the catalyst, (iv) adsorption of at least one reactant on the active sites of the catalyst and (v) surface reaction to yield products.

For the purpose of kinetic study it is important to ensure that the rate data are obtained under the kinetic regime. The experimental conditions are so chosen that the reaction rate is not influenced by external and internal diffusion.

3.2.1. Effect of agitation speed

When a gaseous reactant is used, agitation is of primary importance in facilitating the transport of the gas molecules through the gas–liquid interface. Increasing the agitation until the observed rate remains constant provides conditions under which gas–liquid mass transport is not limiting the reaction. The effect of speed of agitation was studied in the range of 200–1000 rpm. No change was observed in the initial rate beyond a speed of 400 rpm. Thus, the stirring conditions were kept at 400 rpm throughout all the experiments.

3.2.2. Effect of catalyst weight

For a given rate of agitation (400 rpm) and, therefore, a set quantity of hydrogen sulfide available in solution, varying the quantity of catalyst is also a reasonable way of modifying the hydrogen sulfide availability to the catalyst. By plotting the initial rates as a function of the catalyst weight (Fig. 2), a linear dependence is observed until 150 mg of catalyst but the normalized initial rate (i.e. the observed initial rate normalized to the unit weight of catalyst) is not constant which indicates that some transport limitation was present in this reaction.

3.2.3. Effect of particle size

The influence of internal mass transfer on the reaction rate was studied by performing experiments with different particle sizes, while maintaining the same H_2S pressure (5.5 bar), agitation speed (400 rpm), catalyst amount (88 mg) and substrate concentration ([MA] = 0.2 mol l^{-1}). The two mixed magnesium–aluminum oxides tested (KW 2000 and

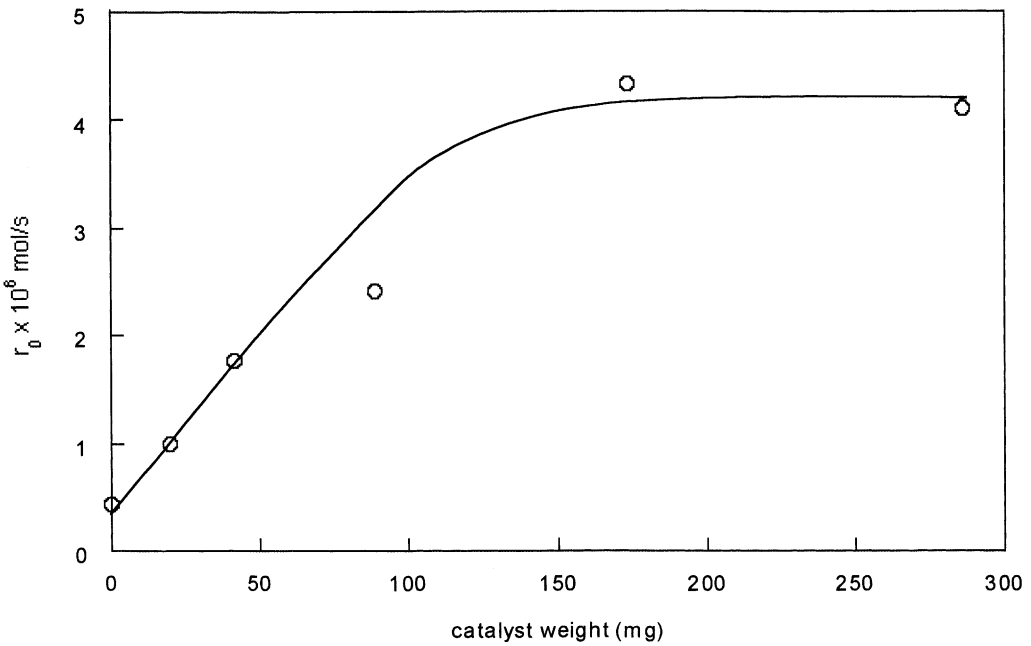

Fig. 2. Plot of the initial reaction rates as a function of the catalyst weight.

Table 1
Initial activity as a function of particle size of KW 2200 catalyst

Particle size (μm)	Surface area ($m^2\,g^{-1}$)	Initial rate ($\times 10^6\,mol\,s^{-1}$)	Specific rate ($\times 10^6\,mol\,s^{-1}\,m^{-2}$)
70	240	3.8	17.7
1.7	160	2.4	17.9

KW 2200) have the same composition but different average particle sizes, 70 and 1.7 μm, respectively. The initial specific activity maintains a steady value ($17.8 \pm 0.1\,mol\,s^{-1}\,m^{-2}$) as shown in Table 1. That means that intraparticle mass transfer resistance is negligible. There is no external or internal mass transfer resistance below an average particle size of 70 μm.

3.2.4. Effect of hydrogen sulfide concentration

Increasing the pressure of the gaseous reactant not only increases the amount of gas present in the gas phase but also increases gas–liquid transport and the solubility of the gas in the liquid phase. The hydrogen sulfide concentration is in equilibrium with the gas phase partial pressure according to the Henry's law:

$$C_{H_2S} = \frac{P_{H_2S}}{H_E}$$

where P_{H_2S} is the partial pressure of H_2S, H_E the Henry's constant and C_{H_2S} is the liquid phase concentration of H_2S at the gas–liquid interface. The dependence of initial rate on initial hydrogen sulfide concentration at fixed initial concentration of methyl acrylate is shown in Fig. 3. As the H_2S pressure is increased, the initial rate increases and then, gradually levels off.

3.2.5. Effect of methyl acrylate concentration

Methyl acrylate initial concentration was varied in the range of 0.1–1.5 $mol\,l^{-1}$, under otherwise similar conditions ($P_{H_2S} = 5.5$ bar), and the initial rate of reaction is plotted as a function of the initial concentration in Fig. 4.

The solubility of the gas phase reactant in the liquid can be influenced by the changes in the concentrations of liquid phase reactant and products. The values

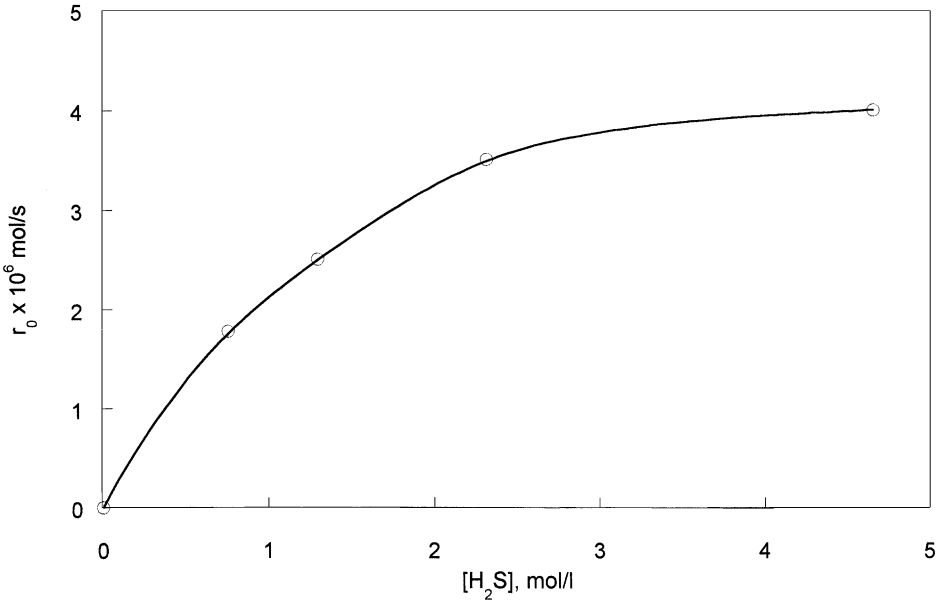

Fig. 3. Plot of the initial reaction rates as a function of the concentration in hydrogen sulfide.

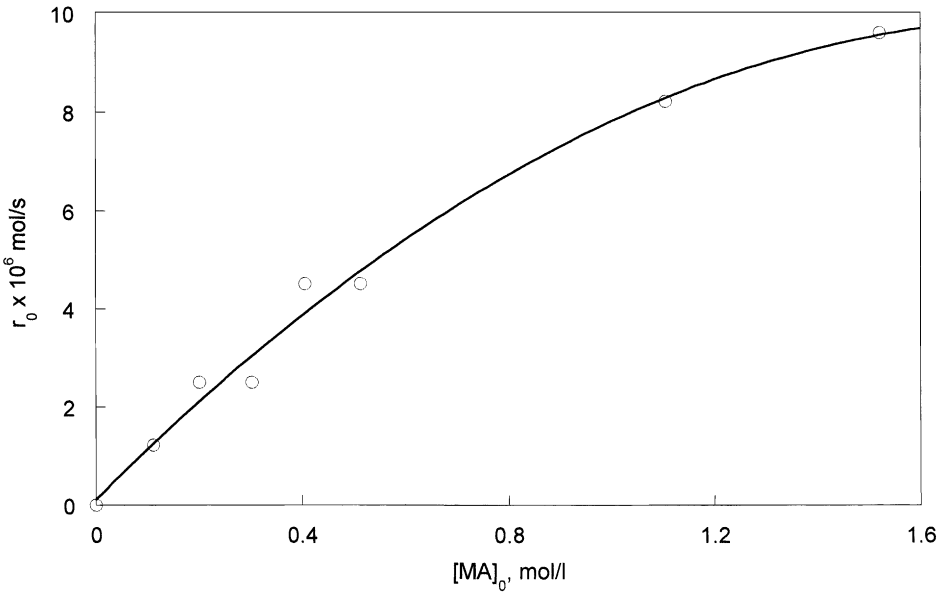

Fig. 4. Plot of the initial reaction rates as a function of the concentration in methyl acrylate.

of Henry's constant determined from experimental solubility data for methyl acrylate, decane and the mixtures are shown in Table 2. As it can be seen, the addition of methyl acrylate to decane solutions significantly increases the solubility of hydrogen sulfide in the mixture.

Hence, this correction factor needs to be considered while interpreting the curve in Fig. 4. Increasing methyl acrylate concentration increases liquid phase hydrogen sulfide concentration and the initial rate is over-estimated.

3.2.6. Effect of methyl 3-mercaptopropionate concentration

For many catalytic systems, the product of a reaction can inhibit the rate of chemical transformation. The inhibition is caused by strong adsorption of the product on the catalyst surface which blocks the actives sites of the catalyst.

When methyl 3-mercaptopropionate (MMP) is initially added together with the reactants, the initial rate of the reaction decreases from 2.5×10^{-6} mol s^{-1} in the absence of MMP to 1.5×10^{-6} mol s^{-1} in the presence of 0.1 mol of MMP added.

Table 2
H_2S solubility in different decane/methyl acrylate mixtures

Decane/methyl acrylate mixture (wt.%)	Henry's constant ($\times 10^2$ mol l^{-1} bar^{-1})
Pure decane	26.1
91/9 (0.8 mol l^{-1} MA)	35
83/7 (1.5 mol l^{-1} MA)	40.4
Pure methyl acrylate (MA)	70.7

3.2.7. Power law model

A simplified representation for the intrinsic kinetics is the power law model, where the rate is presented in terms of an overall rate constant by constants that account for both adsorption and surface reaction. The rate equation based on the power law model is given as:

$$r_0 = k[H_2S]_0^a[MA]_0^b$$

where k, a and b are arbitrary constants valid for a particular system in the range of variables investigated; k is the rate constant and a and b are the reaction orders with respect to hydrogen sulfide and methyl acrylate, respectively.

From the plots of $\log r_0$ versus $\log [H_2S]_0$ at $[MA]_0$ constant and $\log r_0$ versus $\log [MA]_0$ at $[H_2S]_0$

constant, it is possible to determine the values k, a, b, and then the following kinetic law:

$$r_0 = 1.4 \times 10^{-4}[H_2S]_0^{0.4}[MA]_0^{0.8}$$

The fractional orders with respect to H_2S and MA can suggest a competitive adsorption on the catalyst.

The power law model is mathematically simple and is more convenient for fitting the experimental data, but it does not provide insight into the mechanistic aspects of adsorption and surface reaction.

3.3. Kinetic models

For this work, we have developed three models based on different mechanistic assumptions and tested the validity of these models by fitting the proposed rate equations to the experimental rate data. The models chosen were the two most common models proposed in the literature, i.e. a Langmuir–Hinshelwood-type model and an Eley–Rideal-type model. The third model is a modified Eley–Rideal mechanism we have already proposed for various zeolite-catalyzed organic reactions [3,4].

The rate expression for each model is given as follows:

(a) The Langmuir–Hinshelwood model with competitive adsorption of the two reactants on the same type of sites:

$$r_0 = k\frac{K_1[H_2S]_0K_2[MA]_0}{(1 + K_1[H_2S]_0 + K_2[MA]_0)^2} \quad (1)$$

(b) The Eley–Rideal model in which the reaction occurs between the chemisorbed hydrogen sulfide and the liquid phase methyl acrylate in the vicinity of the catalytic site:

$$r_0 = k\frac{K_1[H_2S]_0[MA]_0}{1 + K_1[H_2S]_0} \quad (2)$$

(c) The modified Eley–Rideal model in which the reaction was assumed to proceed between an adsorbed H_2S molecule and a methyl acrylate molecule impacting directly from the liquid bulk phase. The adsorption of methyl acrylate is assumed to be non-neglected. It competes on the adsorption of active sites with H_2S. Such a mechanism can be seen as a modification of the classical Eley–Rideal mechanism and named "poisoned" Eley–Rideal mechanism since MA acts as a poison:

$$r_0 = k\frac{K_1[H_2S]_0[MA]_0}{1 + K_1[H_2S]_0 + K_2[MA]_0} \quad (3)$$

It can be assumed that the surface is covered by H_2S and MA. Eq. (3) then becomes:

$$r_0 = k\frac{K_1[H_2S]_0[MA]_0}{K_1[H_2S]_0 + K_2[MA]_0} \quad (4)$$

By linearizing Eqs. (1), (2) and (4) we obtain Eqs. (5)–(7), respectively:

$$\left(\frac{1}{r_0}\right)^{1/2} = \frac{1 + K_1[H_2S]_0 + K_2[MA]_0}{(kK_1[H_2S]_0K_2[MA]_0)^{1/2}} \quad (5)$$

$$\frac{1}{r_0} = \frac{1}{kK_1[H_2S]_0[MA]_0} + \frac{1}{k[MA]_0} \quad (6)$$

$$\frac{1}{r_0} = \frac{K_2}{kK_1[H_2S]_0} + \frac{1}{k[MA]_0} \quad (7)$$

The discrimination between the three models is done by comparison of the correlation coefficients of the linear regression analyses (Table 3). Model 1 is ruled out from the low correlation coefficient calculated. For models 2 and 3, the correlation coefficients are respectively 0.990 and 0.985, thus the rate expressions of these models can be considered suitable.

In order to distinguish between Eley–Rideal and modified Eley–Rideal mechanisms, we have investigated the competitive adsorption of methyl acrylate and H_2S on the catalytic sites by FT-IR spectroscopy.

3.4. IR results

The IR spectrum of the activated MgO sample shows mainly two ν(OH) bands at 3746 (sharp) and 3623 cm^{-1} (weak) due to residual hydroxyl groups. Coluccia et al. [5] assigned them to OH groups bonded to low coordination sites (corners, steps) and to sites situated on regular planes, respectively.

In order to identify the presence of MMP in the spectra, MMP and MA were first adsorbed separately on the activated MgO catalyst. Fig. 5 presents a spectrum of the species formed upon introduction of a large excess of either MMP or MA followed by evacuation at 313 K. Comparison of both spectra evidences the presence of bands at frequencies such as those situated

Table 3
Correlation coefficients of linear relationship for Langmuir–Hinshelwood and Eley–Rideal kinetic models

Model number	Linear relationship	Correlation coefficient
1	$(1/r_0 \times [MA]_0/[H_2S]_0)^{1/2} = f([MA]_0/[H_2S]_0)$	0.695
2	$1/r_0 = f(1/[H_2S]_0)$	0.990
3	$1/r_0 = f(1/[MA]_0)$	0.985

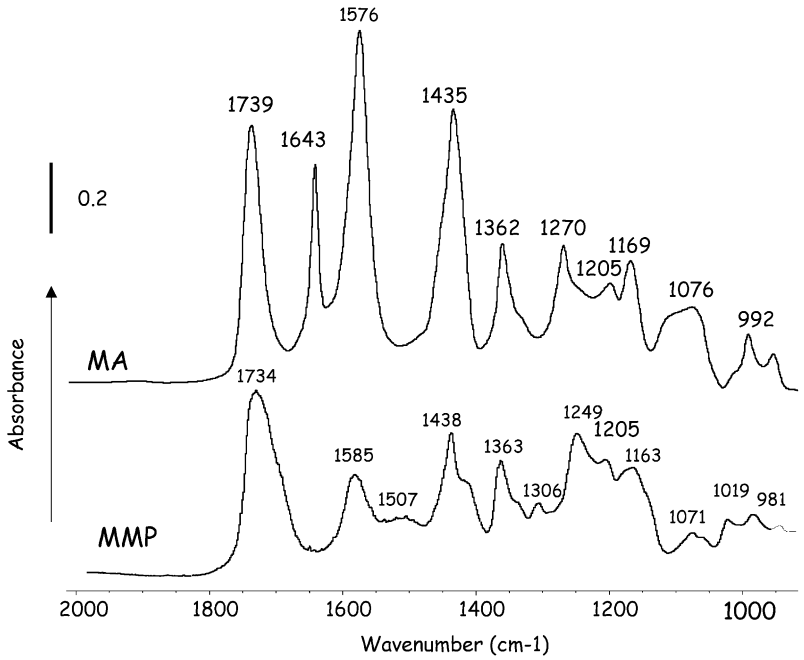

Fig. 5. IR spectra of methyl acrylate (MA) and 3-mercaptopropionate (MMP) (2 Torr at equilibrium followed by evacuation at 313 K) adsorbed on MgO.

near 1735, 1580, 1435, 1360, 1205 and 1165 cm^{-1}. However, the spectrum of chemisorbed MMP presents a particular band at 1249 cm^{-1}, not observed in the case of MA. In the following, this band will be taken as a diagnostic of MMP formation from MA.

Note that before evacuation of MA, additional bands, close to those observed in the liquid state, were detected at 1620, 1404 and 1302 cm^{-1}. They correspond to MA interacting weakly with the surface, or MA physisorbed on MgO.

Two kinds of co-adsorption experiments were further performed which differ in the order of introduction of H_2S and MA. In the first experiment, H_2S in excess (8 Torr at equilibrium) was introduced first onto the activated MgO pellet. The spectrum shows the formation of a very broad ν(OH) band at 3496 cm^{-1} and of a weak ν(SH) one near 2589 cm^{-1} accompanied by two shoulders at about 2580 and 2575 cm^{-1} [6]. The formation of new OH and SH groups clearly provides evidence for the dissociative adsorption of a part of H_2S (Scheme 2).

After H_2S evacuation at 313 K, MA (2 Torr at equilibrium) was introduced. Spectra were recorded after

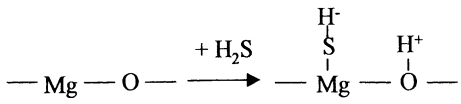

Scheme 2. Dissociative adsorption of H_2S over MgO.

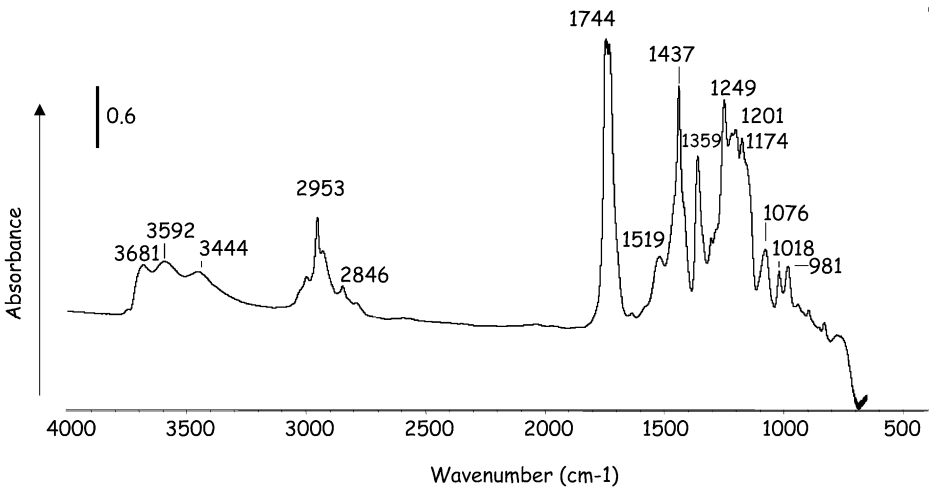

Fig. 6. IR spectrum of the species formed from the co-adsorption of H_2S (8 Torr of H_2S adsorbed and evacuated at 413 K) followed by introduction of MA (2 Torr of MA) after 30 min of contact with MgO.

different contact times. Fig. 6 presents the spectrum of species formed after 30 min of contact time. MMP appeared, as shown by the presence of the band at 1249 cm^{-1}.

The reverse experiment was also performed: MA was firstly introduced and evacuated at 313 K, then 8 Torr of H_2S at equilibrium were added (Fig. 7A). In this case, no clear presence of MMP can be detected since the band at 1249 cm^{-1} is hardly visible. After such an experiment, MA (2 Torr at equilibrium) was added at 313 K, without any previous evacuation of the excess of H_2S. Fig. 7B provides clear evidence for the formation of MMP.

Finally, addition of an excess of MA (2 Torr at equilibrium) on MgO followed by addition of H_2S (8 Torr at equilibrium) leads to the formation of MMP (band

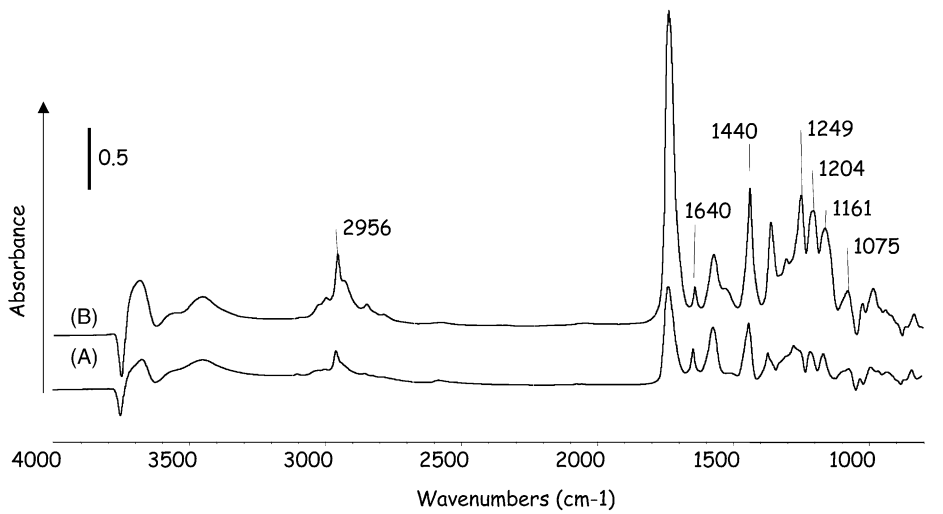

Fig. 7. IR spectra of the species formed from the co-adsorption of MA and H_2S on MgO: (A) 2 Torr of MA adsorbed and evacuated at 313 K, followed by introduction of 8 Torr of H_2S; (B) (A) followed by the addition of 2 Torr of MA.

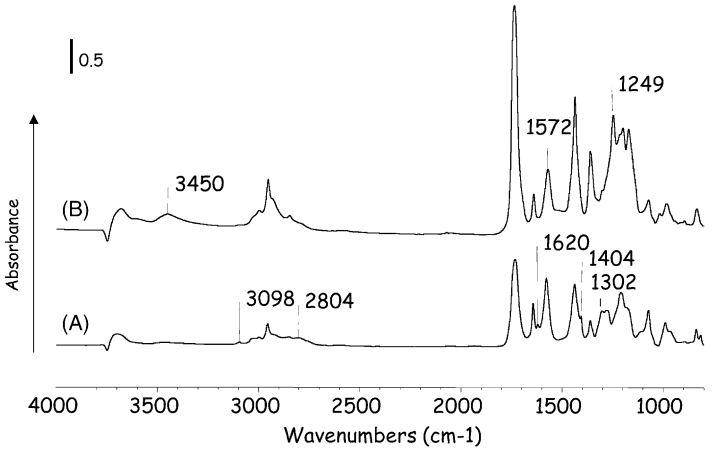

Fig. 8. IR spectra of the species formed from the (A) adsorption of 2 Torr of MA (without evacuation) on MgO, (B) (A) followed by the addition of 8 Torr of H_2S.

at 1249 cm^{-1}) (Fig. 8B). Recording MMP signal versus time (spectra not shown) reveals that its formation occurs at the expense of weakly adsorbed MA species. Indeed, the comparison of Fig. 8A and B, shows that the bands at 1620, 1404 and 1302 cm^{-1} present before H_2S introduction disappear when H_2S is added.

This IR study then allows evidencing that the formation of methyl 3-mercaptopropionate occurs through the reaction between methyl acrylate and HS^- species resulting from H_2S dissociative adsorption on MgO (Fig. 6). No reaction occurs when only strongly chemisorbed MA species are in contact with an excess of H_2S (Fig. 7A) while MMP formation is observed when MA is present in excess (Fig. 7B and 8). This allows us to show that physisorbed MA species reacts with HS^- species to form MMP.

4. Conclusion

Combined kinetic analysis and IR spectroscopic studies suggest that, among the models considered, a "poisoned" Eley–Rideal-type model gives the best description of the mechanism of addition of H_2S to methyl acrylate over solid basic catalysts. The rate-determining step is the surface reaction between adsorbed hydrogen sulfide and physisorbed methyl acrylate. The IR study of the reaction of H_2S and MA on MgO completely agrees with the results issued from the kinetic modeling.

Acknowledgements

The Groupement de Recherches de Lacq is gratefully acknowledged for financial support.

References

[1] Y. Hino, T. Wakao, T. Hayashi, T. Ishikawa, JP 6,298,724, KK Nippon Shokubai (1994).
[2] E. Arretz, Fr. Dem. 96-14299, Elf-Atochem, 1996.
[3] N. Barthel, A. Finiels, C. Moreau, R. Jacquot, M. Spagnol, J. Mol. Catal. A: Chem. 169 (2001) 163.
[4] P. Moreau, A. Finiels, P. Méric, J. Mol. Catal. A: Chem. 154 (2000) 185.
[5] S. Coluccia, L. Marchese, S. Lavagnini, M. Anpo, Spectrochim. Acta 43A (1987) 1573.
[6] O. Manoilova, Ph.D. Thesis, University of Caen, 2002.